Causal effect of disconnection lesions on interhemispheric functional connectivity in rhesus monkeys

Jill X. O'Reilly[a,1,2], Paula L. Croxson[b,1,2], Saad Jbabdi[a], Jerome Sallet[c], MaryAnn P. Noonan[d], Rogier B. Mars[a,c], Philip G. F. Browning[b], Charles R. E. Wilson[e], Anna S. Mitchell[c], Karla L. Miller[a], Matthew F. S. Rushworth[a,c], and Mark G. Baxter[b]

[a]Functional Magnetic Resonance Imaging of the Brain Centre, Nuffield Department of Clinical Neurosciences, John Radcliffe Hospital, Oxford University, Oxford OX3 9DU, United Kingdom; [b]Glickenhaus Laboratory of Neuropsychology and Friedman Brain Institute, Department of Neuroscience, Icahn School of Medicine at Mount Sinai, New York, NY 10029; [c]Department of Experimental Psychology, Oxford University, Oxford OX1 3UD, United Kingdom; [d]Oxford Centre for Human Brain Activity, University Department of Psychiatry, Warneford Hospital, Oxford University, Oxford OX3 7JX, United Kingdom; and [e]Stem Cell and Brain Research Institute, Institut National de la Santé et de la Recherche Médicale Unité 846, 69675 Bron, France

Edited by Robert Desimone, Massachusetts Institute of Technology, Cambridge, MA, and approved July 15, 2013 (received for review March 19, 2013)

In the absence of external stimuli or task demands, correlations in spontaneous brain activity (functional connectivity) reflect patterns of anatomical connectivity. Hence, resting-state functional connectivity has been used as a proxy measure for structural connectivity and as a biomarker for brain changes in disease. To relate changes in functional connectivity to physiological changes in the brain, it is important to understand how correlations in functional connectivity depend on the physical integrity of brain tissue. The causal nature of this relationship has been called into question by patient data suggesting that decreased structural connectivity does not necessarily lead to decreased functional connectivity. Here we provide evidence for a causal but complex relationship between structural connectivity and functional connectivity: we tested interhemispheric functional connectivity before and after corpus callosum section in rhesus monkeys. We found that forebrain commissurotomy severely reduced interhemispheric functional connectivity, but surprisingly, this effect was greatly mitigated if the anterior commissure was left intact. Furthermore, intact structural connections increased their functional connectivity in line with the hypothesis that the inputs to each node are normalized. We conclude that functional connectivity is likely driven by corticocortical white matter connections but with complex network interactions such that a near-normal pattern of functional connectivity can be maintained by just a few indirect structural connections. These surprising results highlight the importance of network-level interactions in functional connectivity and may cast light on various paradoxical findings concerning changes in functional connectivity in disease states.

resting-state connectivity | macaque | fMRI | split brain

Resting-state functional connectivity [intrinsic correlations in activity between brain areas, measured in the absence of overt stimulation or task demands (1, 2)] provides a powerful tool for understanding the global organization of the brain (3–6), charting its connectional structure (e.g., refs. 7–11), and detecting brain changes in disease. Functional connectivity changes have been identified in diverse conditions including Alzheimer's disease (6, 12–14), Parkinson's disease (15, 16), multiple sclerosis (17, 18), autism (19), depression (20, 21), and schizophrenia (22, 23).

To relate changes in functional connectivity to physiological changes in the brain, it is important to understand how functional connectivity depends on the physical integrity of brain tissue. However, there is a disparity in the conclusions that have been drawn from work on the healthy brain and patient studies. It is generally accepted that in the healthy brain, functional connectivity correlates with structural connectivity (the presence and integrity of white matter connections) (3, 24, 25), and computational modeling suggests that structural connectivity shapes and constrains functional connectivity (3, 24). However, the data from patient populations, which should provide the clearest evidence of a causal and necessary link between structural and functional connectivity, remain equivocal. Reduced structural connectivity in the brain does not necessarily lead to decreased functional connectivity. In patients with white matter damage (multiple sclerosis), decreases in structural connectivity have been observed to correlate with increases in functional connectivity (17). Even more striking is that normal levels of interhemispheric functional connectivity persist in individuals totally lacking the normal corticocortical white matter connection between hemispheres: individuals born without a corpus callosum (callosal agenesis) (26) and patients with surgical lesions of the corpus callosum (27).

In light of the observations that functional connectivity can persist when structural connectivity is compromised or absent, the assumption that corticocortical white matter tracts constrain and define the pattern of functional connectivity in the brain is called into question. Alternative hypotheses have been proposed: One suggestion is that correlated patterns of functional connectivity and structural connectivity are set up independently and in parallel, driven by external forces such as shared sensory input and shared task involvement of correlated areas (26). Another possibility is that subcortical structures such as the thalamus or the superior colliculus play a greater role than previously thought in defining the flow of information between cortical regions (28, 29).

To test whether the relationship between (corticocortical) structural connectivity and functional connectivity is causal or only correlative, data from individuals with white matter damage are essential. An ideal model system is section of the corpus callosum because the corpus callosum forms the sole direct structural connection between most parts of the two cerebral hemispheres; studies of other white matter tracts are complicated by the fact that in general, when a white matter connection

Author contributions: J.X.O., P.L.C., C.R.E.W., and M.G.B. designed research; P.L.C., J.S., M.P.N., R.B.M., P.G.F.B., C.R.E.W., and A.S.M. performed research; J.S. performed histological work; P.G.F.B. performed the neurosurgery; K.L.M. contributed new reagents/analytic tools; J.X.O., P.L.C., S.J., R.B.M., and M.F.S.R. analyzed data; and J.X.O., P.L.C., M.F.S.R., and M.G.B. wrote the paper.

The authors declare no conflict of interest.

This article is a PNAS Direct Submission.

Freely available online through the PNAS open access option.

[1]J.X.O. and P.L.C. contributed equally to this work.

[2]To whom correspondence may be addressed. E-mail: joreilly@fmrib.ox.ac.uk or paula.croxson@mssm.edu.

This article contains supporting information online at www.pnas.org/lookup/suppl/doi:10.1073/pnas.1305062110/-/DCSupplemental.

between two regions is damaged, alternative structural connection pathways remain, and these indirect connections may support continued functional connectivity (30).

Unfortunately, evidence from studies of acallosal human subjects is equivocal: although one recent study of individuals with callosal agenesis provided particularly strong evidence for normal interhemispheric functional connectivity in a relatively large cohort (eight patients) and is supported by evidence from a case study of surgical section of the corpus callosum (27), other studies with smaller numbers of patients have reported that functional connectivity is disrupted in callosal section or agenesis (31, 32). Interpretation of patient studies is complicated for several reasons. First, these studies have used different patient groups (surgical disconnection vs. callosal agenesis; in the latter, noncallosal commissures may be enlarged), although disruption and retention of connectivity have been observed in both groups (26, 27, 31, 32). Second, the surgical disconnection patients were not neurologically typical even before surgery since they suffered from epilepsy (17, 23). Third, many of the patients may have developed compensatory connections as a result of the patient developing without a corpus callosum or a large amount of time elapsing between the surgical disconnection and the resting-state scan (22, 23, 26).

We probed the relationship between structural and functional connectivity using a controlled, experimental approach in macaque monkeys. We gave macaque monkeys a complete section of the corpus callosum, either with or without section of the anterior commissure, and compared their resting-state functional connectivity 8 mo after the lesion to functional connectivity in the same subjects before the lesion and to a group of 18 normal control monkeys. We show here that the corpus callosum section disrupts interhemispheric functional connectivity if the anterior commissure is also sectioned. However, functional connectivity across the whole network was preserved in the case in which the anterior commissure was spared. Our findings confirm the strong link between functional and structural connectivity but also provide evidence for a complex relationship between even minor structural connections and widespread functional connectivity.

Results

We collected resting-state functional magnetic resonance imaging (fMRI) and structural scans from three rhesus macaque monkeys, before and after complete section of the corpus callosum. All three monkeys (monkeys N, P, and R) received complete lesions of the corpus callosum. In two of the monkeys (monkeys N and P), the anterior commissure was also sectioned; in the third monkey (monkey R), the anterior commissure remained intact. We refer to these lesions throughout the paper as "AC + CC" and "CC only." For histology of the lesions, see Fig. 3. Additionally, resting-state fMRI data were collected using the same protocol from 18 control monkeys, which had no lesion.

Resting functional data were collected presurgery and postsurgery, under light isoflurane anesthesia in accordance with veterinary advice, in conditions under which resting activity has previously been observed in macaque monkeys (33). We have used this protocol in previous functional connectivity work in macaques and observed patterns of functional connectivity similar to those that are observed in awake, resting humans (34, 35). Protocols for data collection and preprocessing are described in *Materials and Methods*.

We projected the fMRI data onto the surface of a macaque brain template (the F99 brain) with 20,000 vertices. Data at each vertex were normalized, and the mean activity over the entire surface was regressed out at each vertex. Data were then summarized by one time series of activity for each of 56 Brodmann areas (28 in each hemisphere), defined as the mean of all voxels' time series within that region. The Brodmann regions were defined using the Brodmann macaque atlas (36), transcribed into the space of the F99 brain template (37), and implemented in CARET (Computerized Anatomical Reconstruction and Editing Toolkit) (38).

Interhemispheric Connectivity Was Significantly Reduced Postlesion Across the Group. To investigate the changes in interhemispheric functional connectivity following disconnection of the hemispheres, we constructed matrices of the pairwise correlation between brain regions, again using the 56 (28 × 2) regions from the Brodmann atlas.

Matrices of mean correlation scores (Gaussianized as Fisher's *z*) for the three monkeys, prelesion and postlesion, are shown in Fig. 1 *A* and *B*; the same data for the control group are shown in Fig. S1. It is striking on inspection of the data that although the prelesion pattern of interhemispheric functional connectivity resembles intrahemispheric functional connectivity, postlesion interhemispheric functional connectivity is largely abolished.

To aid visualization, we defined four functional "blocks"—clusters of regions that were correlated within each hemisphere. These blocks were defined by *k*-means clustering on the Brodmann areas' time courses within each hemisphere, pooling

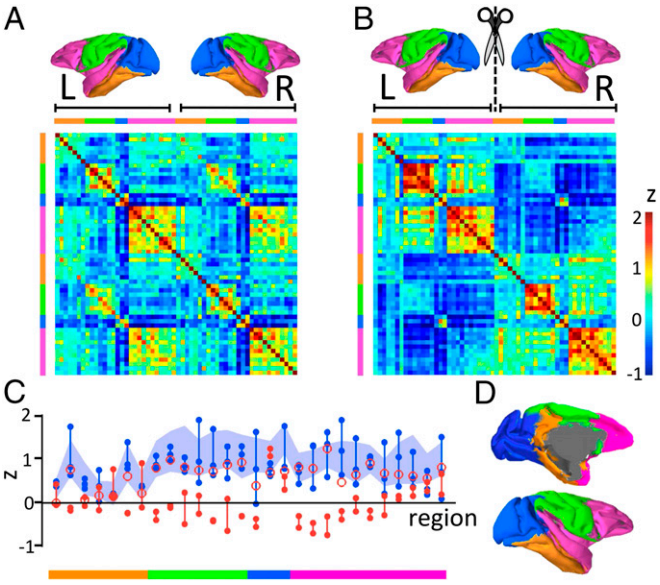

Fig. 1. Matrices of connectivity (Fisher's *z*), prelesion and postlesion. (*A* and *B*) Brodmann areas are presented in the same order for LH and RH, so that the main diagonal shows the correlation of each region with itself, the upper left and lower right quadrants show correlations within hemispheres, and the lower left and upper right quadrants show interhemispheric connectivity. Color scale ranges from $z = -1$ to $z = 2$ in both cases. For visualization purposes, we grouped regions into four correlation blocks (*k*-means clustering within hemisphere, across all subjects and sessions). The colored key above and beside each matrix indicates to which block the columns belong. The four correlation blocks are indicated on the small brain images. (*C*) Dots indicate Fisher's *z* for correlation between homotopic regions in the three individuals, prelesion (blue) and postlesion (red). The shaded area is the mean ± 2 SD for a group of 18 control monkeys. The postlesion data from monkey R (CC-only lesion; intact anterior commissure) is illustrated by open red circles—the level of interhemispheric connectivity in this monkey, postlesion, is significantly above zero and resembles the prelesion data from all three monkeys and the control data. The regions in the blue block which retain strong interhemispheric connectivity in all monkeys are V1 and V2; this effect could be driven by smoothing of the fMRI data across the midline or by passing of visual information via subcortical routes including the superior colliculus (61, 62). (*D*) Location of the connectivity blocks displayed on the f99 brain template.

all scans (prelesion and postlesion); details are given in *SI Materials and Methods*. Note that the purpose of defining these functional blocks was purely illustrative: the intention was to make Figs. 1 and 2 easier to interpret by labeling within-hemisphere correlated regions in the same color. The clustering analysis was explicitly not performed with the intention of drawing conclusions about the organization of functional connectivity within hemispheres, about which there exist numerous studies (e.g., refs. 5 and 39).

To provide statistical tests of the changes in correlation between hemispheres postlesion, we entered the values of Fisher's z for each pair of homotopic regions (each region and its contralateral homolog, e.g., left auditory cortex and right auditory cortex; these pairs are represented on the leading diagonal of the upper right and lower left quadrants of the connectivity matrix) for each monkey into a repeated-measures ANOVA (repeated measures were the prelesion and postlesion values of Fisher's z for each of the 28 different region pairs; between subjects, variability was also modeled). There was a significant main effect of prelesion vs. postlesion on connectivity between homotopic regions across the group ($F_{2, 165} > 10.5$, $P < 0.00005$). The correlations (Fisher's z) between homotopic pairs in each monkey, prelesion, postlesion, and in the control group, are plotted in Fig. 1*C*.

Multidimensional Scaling Reveals a Striking Impact of Corpus Callosum Lesion Across the Group. To further visualize the global changes in functional connectivity patterns prelesion and postlesion, we applied a multidimensional scaling analysis to the correlation data from the group of three monkeys. Multidimensional scaling is a visualization technique in which data points that are distributed in high-dimensional space are remapped to a low-dimensional space (in this case, 2D) in such a way that points which are close together in the original data space remain close in the "similarity space" (the 2D visualization). In the present case, the high-dimensional data set we wished to visualize consisted of the pairwise similarity between time courses for each pair of Brodmann regions.

The results of the multidimensional scaling analysis are shown in Fig. 2. Clearly, the dominant pattern of organization shifts from functional blocks of paired regions (before the lesion) to two separate networks, with component functional blocks (after section of the corpus callosum). In other words, when the corpus callosum is intact, each region is closely correlated with its contralateral homolog (Fig. 2*A*) and its functional block; afterward, the lesion regions and their contralateral homologs are much less closely correlated (Fig. 2*B*), although functional blocks within each hemisphere are maintained. Conversely, before the lesion, the data points for the two hemispheres overlap in similarity space; after the lesion, two separate clusters are formed for the two separate hemispheres (Fig. 2 *C* and *D*).

Note that the results of the multidimensional scaling are described only qualitatively because multidimensional scaling is a visualization technique rather than a statistical analysis; these results should therefore be considered an illustration of the statistical tests presented in the previous section.

Sparing of the Anterior Commissure Resulted in Surprisingly Widespread Sparing of Interhemispheric Functional Connectivity. Notably, the reduction in interhemispheric functional connectivity was much less severe in the monkey with intact anterior commissure (monkey R; CC-only lesion) than in the other two monkeys (monkeys N and P; AC + CC lesion). Data from this monkey are indicated by open red circles in Fig. 1*C*. The difference between the effects of AC + CC and CC-only lesions can also be seen in the individual functional connectivity matrices (Fig. 3) and in the plots of the distribution of interhemispheric functional connectivity across the cortex (Fig. 4; raw difference in correlations is shown in Fig. S2).

Statistically, there was a significant interaction between session (prelesion vs. postlesion) and monkey ($F_{2, 165} = 4.3$, $P = 0.015$) in the repeated measures ANOVA reported above; post hoc tests confirmed that the magnitude of reduction in interhemispheric connectivity was less in monkey R (CC only) than in monkeys N and P (AC + CC).

In all monkeys, there was a within-subjects reduction in interhemispheric connectivity from prelesion to postlesion scan (paired-samples t test comparing Fisher's z for 28 pairs of homotopic regions in each monkey prelesion and postlesion resulted in $t_{27} = -5.9$, -6.0, and -4.6 and $P = 0.000013$, 0.0000098, and 0.00004023 for monkeys N, P, and R, respectively). However, the magnitude of the reduction was less after CC-only lesion [mean change in Fisher's z across pairs of homotopic regions was 0.34 in monkey R (CC only) and 0.91 and 0.62 in monkeys N and P (AC + CC)]. The mean values of Fisher's z for homotopic pairs, prelesion and postlesion, illustrate the greater change after AC + CC lesion (for monkey N, prelesion = 0.90 and postlesion = −0.0045; for monkey P, prelesion = 0.57 and postlesion = −0.044) than in CC-only lesion (for monkey R, prelesion = 0.97 and postlesion = 0.62).

Comparison with a group of 18 control monkeys allowed us to determine the distribution of the lesion effect, i.e., to determine which parts of cortex were most disconnected after the lesions. We calculated t statistics for postlesion interhemispheric functional connectivity (Fisher's z for each pair of homotopic Brodmann regions in the postlesion scan, compared with 18 control monkeys) in each region in monkeys N, P, and R. In Figs. 3*C* and 4, it can be seen that after AC + CC lesion (monkeys N and P), most Brodmann regions had significantly lower interhemispheric functional connectivity compared with the group of 18 controls. In contrast, after CC-only lesion (monkey R), only one region (visual area V2) showed a (barely) significant change in

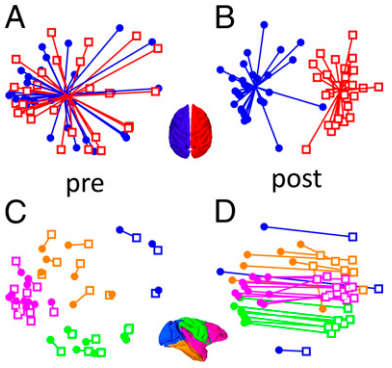

Fig. 2. Multidimensional scaling plots. These plots illustrate the correlation between Brodmann areas in resting-state data, before and after corpus callosum lesion (using averaged correlations for the three monkeys). (*A* and *C*) Prelesion and (*B* and *D*) postlesion (note that the data points in each pair of plots are identical). Each Brodmann region is represented by a dot (circles for LH and squares for RH). Dots are arranged (by MD scaling) such that the distance between each pair of dots is proportional to their dissimilarity (inverse correlation as defined in the main text). Therefore, dots that are closer together represent regions with stronger functional connectivity. In *A* and *B*, regions are colored by hemisphere (blue circles, LH; red squares, RH). Each region is linked to the mean position in the scaled (illustrated) space for its hemisphere; note that before the lesion, the networks for the two hemispheres are heavily overlapping, but after the lesion, they move apart. In *C* and *D*, the same data are presented as in *A* and *B*, but now each area is linked to its homotopic counterpart in the contralateral hemisphere, and areas are colored according to the within-hemisphere blocks (defined by *k*-means clustering; *Materials and Methods*). Note that before the lesion, there is strong pairwise organization with each pair of homotopic regions falling close together in scaled space; after the lesion, the pairs are separated.

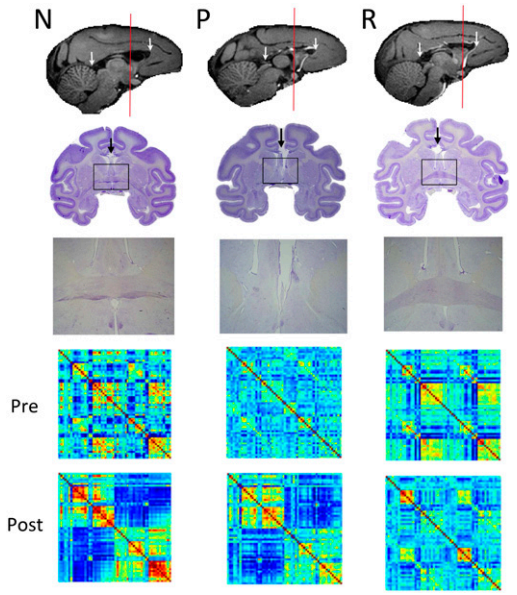

Fig. 3. Effect of anterior commissure sparing. Each column corresponds to one monkey. anterior commissure section was attempted in monkeys N and P but not monkey R. The first row shows T1-weighted anatomical MRI scans (sagittal view of the midline) showing the extent of the corpus callosum section. The anterior and posterior limits of the section are shown by white arrows. The corpus callosum was fully sectioned in all three monkeys. The second row shows a coronal brain slice stained with Cresyl Violet. The slice was taken at the level of the posterior extent of the arcuate sulcus (~18 mm anterior to the interaural line, according to ref. 63; shown by the red line on the T1 images) and shows the corpus callosum (black arrow) and anterior commissure (inside black box). The third row shows a close up on the anterior commissure from the same slice (shown by the black box on each slice). In monkey N the anterior commissure was sectioned, with just a few fibers spared. Monkey P had a complete section of the anterior commissure, as evidenced by the complete degeneration of the fibers. Monkey R had a completely intact anterior commissure. The fourth and fifth rows show matrices of values of Fisher's *z* for each pair of regions. These matrices are the same as in Fig. 2, but here data for each monkey are presented separately. Note that interhemispheric connectivity is more intact in monkey R, in which the anterior commissure was also intact.

interhemispheric functional connectivity, compared with the group of 18 controls.

Primary Visual Cortex Connectivity Is Partially Spared Postlesion. An exception to the overall pattern of results was observed in the primary visual cortex (V1), in which interhemispheric connectivity was preserved postlesion (Fig. 4; also note the "hot spot" of preserved interhemispheric connectivity in Figs. 1 and 3). Comparison of postlesion scans with the control group of 18 monkeys indicates no significant effect of lesion on interhemispheric connectivity in V1 ($P > 0.05$ for all monkeys). It is possible that the shared time course of activity in left and right V1 may have been driven by shared visual input (although the monkeys' eyes were closed during scanning, light does pass through the eyelids and would be in phase in both eyes).

Intrahemispheric Functional Connectivity Increases After Corpus Callosum Section. In addition to our main findings, we were surprised to note, on inspection of the connectivity matrices, that intrahemispheric functional connectivity appears to increase after the disconnection of the hemispheres by lesion of the corpus callosum and anterior commissure. Again, this effect was greatly mitigated by sparing of the anterior commissure. We carried out paired-samples *t* tests on the value of Fisher's *z* for each pair of nonhomotopic regions within each hemisphere; i.e., values of Fisher's *z* for 756 = 27 × 28 pairs of regions (all possible within-hemisphere pairings) in each hemisphere in each monkey were entered into paired-samples *t* tests for prelesion vs. postlesion functional connectivity. After AC + CC lesion, in both hemispheres, there was a significant increase in within-hemisphere functional connectivity postlesion [mean change in values of Fisher's *z* in monkey N was +0.29 and +0.35 for left hemisphere (LH) and right hemisphere (RH), and for monkey P it was +0.49 and +0.24 for LH and RH; $t_{755} < -3.9$ and $P < 0.0005$ for both hemispheres in both monkeys N and P]. In contrast, after CC-only lesion, there was a very small decrease in within-hemisphere functional connectivity postlesion: for monkey R, the mean change in Fisher's *z* was −0.069 and −0.026 for LH and RH; $t_{755} = 2.8$ (LH) and 0.75 (RH), and $P = 0.0027$ (LH) and 0.23 (RH). This effect is not significant for the RH; for the LH it is barely significant after Bonferroni correction for hemispheres × monkeys (significant for $\alpha = 0.05$ but not for $\alpha = 0.01$). In conclusion, there was a significant increase in intrahemispheric functional connectivity after the lesion of corpus callosum and anterior commissure but little or no change after corpus callosum lesion only.

Discussion

We have presented evidence for a causal relationship between structural and resting-state functional connectivity. In macaque monkeys with section of the corpus callosum, our resting-state fMRI results show that disconnection of the interhemispheric corticocortical white matter connections (corpus callosum and anterior commissure) causes near-total abolition of functional connectivity between the cerebral hemispheres. This result provides strong evidence that corticocortical white matter connections are indeed necessary for the propagation of resting-state activity between cortical regions.

However, two further observations speak against a straightforward one-to-one mapping between structural and functional connectivity. These observations concern (*i*) the surprisingly strong and widespread preservation of interhemispheric functional connectivity in a monkey with intact anterior commissure and (*ii*) changes in intrahemispheric connectivity following disconnection of the hemispheres.

Sparing of the anterior commissure resulted in a surprising magnitude and extent of spared interhemispheric functional connectivity, suggesting that the number and directness of structural connections may not be the key factor driving functional

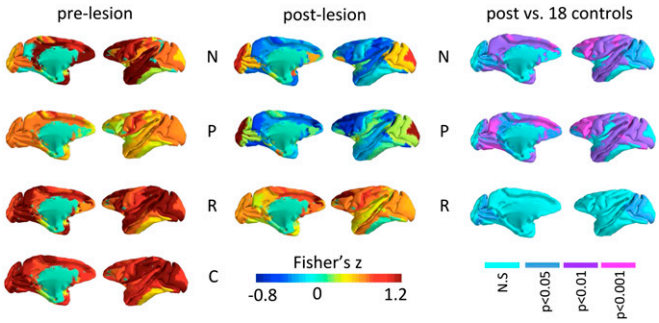

Fig. 4. Distribution of interhemispheric functional connectivity prelesion and postlesion. The figure shows the 28 Brodmann areas, colored by the value of Fisher's *z* (Gaussianized correlation score) between each region and its homotopic counterpart in the other hemisphere. Each row represents a monkey (the figure labeled C in the prelesion column is the average of 18 control monkeys). Note the widespread decrease in interhemispheric functional connectivity in monkeys N and P (AC + CC lesion) but not in monkey R (CC only; intact anterior commissure). Right column shows *P* values for interhemispheric connectivity in postlesion scan vs. 18 controls.

connectivity. Although full section of the forebrain commissures (AC + CC) resulted in the near-total abolition of interhemispheric functional connectivity, the effect after CC-only lesion was significantly smaller—indeed, interhemispheric connectivity remained within the normal range defined in terms of a group of 18 control monkeys. In other words, a small proportion of the structural connections (those carried in the anterior commissure) were able to maintain a large proportion of the functional connectivity.

It is intriguing that although the anterior commissure carries interhemispheric structural connections between only a subset of areas [the temporal lobes, the orbitofrontal cortex, and amygdalae (40)], interhemispheric functional connectivity was maintained between a much wider set of regions, including those (e.g., parietal cortex and dorsolateral prefrontal cortex) with no anterior commissure projections (Fig. 4). The contrast between the structural connections of the anterior commissure and the map of intact interhemispheric connectivity in monkey R is illustrated in Fig. S3. The anterior commissure in monkeys has been shown to be responsible for a large amount of visual and mnemonic transfer between the hemispheres (41, 42). We note that the anterior commissure is substantially larger in rhesus monkeys than in humans: around 5% of area of the corpus callosum as opposed to 1% in humans (43). However, humans with an intact anterior commissure also have preserved interhemispheric transfer of information (44).

Our results indicate that although recent studies in acallosal human subjects reported intact interhemispheric functional correlations (26), this effect need not imply a dissociation between structural and functional connectivity. Instead, preserved functional connectivity could be explained in terms of the existence of noncallosal commissures, particularly the anterior commissure. Indeed, noncallosal connections may even be enlarged in callosal agenesis: developmental pruning of axonal projections in the ACs is reduced in monkeys in whom the corpus callosum does not develop (45), whereas in genetically modified mice with agenesis of the corpus callosum, the number of unmyelinated fibers in the anterior commissure is increased (46). Furthermore, people with callosal agenesis often display additional interhemispheric connections in the form of sigmoidal white matter bundles that connect the frontal lobe to the contralateral occipital lobe (47) and are not present in neurotypical subjects.

More generally, the present results, taken together with the studies on human patients (26, 27), indicate that even weak and indirect connections between the hemispheres are enough to maintain interhemispheric functional connectivity. This finding supports a hypothesis from modeling work: Adachi et al. (30) modeled the effect of different types of indirect connections on functional connectivity in macaque monkeys. They found that surprisingly, functional connectivity between pairs of regions without a direct corticocortical connection depended more strongly on whether the two regions (a and b) had common inputs and outputs (a ← c → b; a → c ← b) than on whether there was (two-step) information flow between them (a → c → b). Hence, they hypothesized that functional connectivity depends more strongly on network level than on pairwise interactions. The present results support that view.

An additional observation, concerning changes in intrahemispheric functional connectivity, also has implications for our understanding of functional connectivity in terms of networks rather than bilateral connections. On complete disconnection of the hemispheres (AC + CC lesion), correlations between regions within each hemisphere actually increased. This finding is compatible with a framework of input normalization (where the effect of each input on a given region is scaled by the total number of regions) and with previous theoretical work: In a brain-like network, simulations indicate that although lesions decrease functional connectivity along pathways which are immediately damaged, parallel pathways actually increase their connectivity (48). This observation offers a potential explanation for "paradoxical" results in which functional connectivity between some regions increases in disease or predisease states, including in early-stage multiple sclerosis (17) and in carriers of the *APOE4* allele, a genetic risk factor for Alzheimer's disease (12, 49).

Overall, although our results support the general assumption that functional connectivity depends on structural connectivity and is not entirely driven by, for example, shared sensory input, they also reveal two interesting features of functional connectivity networks. First, it appears that these networks are sufficiently stable such that even weak connections between a subset of areas in LH and RH sections of each network are enough to maintain relatively strong correlations across almost the entire bilateral network. Second, the loss of some structural connections may increase functional connectivity via other routes. It is worth considering, therefore, that there is not a one-to-one mapping between the existence of pairwise structural connections and functional connectivity patterns.

The concept of disconnection has long been important in neurology (50–52), and several of the major neurological syndromes, including aphasia (50, 53), amnesia (54), and neglect (55, 56), can result from white matter damage rather than damage to the cortical gray matter. In that context, resting-state functional connectivity could provide a useful tool for determining the nature of the functional network retained after white matter damage, for example, in stroke, and targeting therapies accordingly (57, 58). However, even in the simple case presented here, the strength of functional connectivity between each pair of nodes is not a linear function of the strength of direct structural connections between them because partial loss of structural connectivity does not necessarily cause a partial loss of functional connectivity. Furthermore, network effects, as well as bilateral structural connectivity, contribute to functional connectivity patterns. It therefore seems that a greater understanding of network interactions will be an important step in the translation of resting-state fMRI from laboratory to clinic.

Materials and Methods

Monkeys and Lesions. We collected resting-state fMRI and structural scans from three rhesus macaque monkeys (*Macaca mulatta*): one male (R) and two female (N and P) with ages ranging from 3 to 6 y at the time of the preoperative MRI scan. The monkeys were socially housed in different troops. All monkeys received complete lesions of the corpus callosum including the genu and the splenium. The hippocampal commissures and the fornix were spared in all cases. In two of the three monkeys (monkeys N and P) the anterior commissure was successfully sectioned, and in the third monkey (monkey R) it was left intact. All three monkeys received a preoperative MRI scan 3 wk before surgery and a postoperative MRI scan 8 mo following surgery. We also collected resting-state fMRI and structural scans from a further 18 rhesus macaque monkeys (the control group) using the same protocol.

MRI Data Acquisition and Analysis. We collected fMRI data under light isoflurane anesthesia, using a previously published protocol (34, 35). Details are given in *SI Materials and Methods*.

Data were acquired in a 3-T MRI scanner with a full-size bore using a four-channel phased-array coil (H. Kolster, Windmiller Kolster Scientific, Fresno, CA), using a previously described protocol, which is redescribed in *SI Materials and Methods*. We acquired 1,600 volumes (53 min) of functional data. fMRI data were analyzed using tools from Oxford Centre for Functional Magnetic Resonance Imaging of the Brain (FMRIB) Software Library (59, 60), FMRIB in-house software, and MATLAB. Data were preprocessed in the following steps: removal of nonbrain matter from images, removal of head motion artifacts by linear regression (MCFLIRT), Gaussian spatial smoothing (FWHM 3 mm), temporal band-pass filtering between 0.01 and 0.05 Hz (to reduce noise from scanner drift and respiration, respectively), manual identification of noise components (from vasculature, respiration, and head motion) using independent components analysis (MELODIC), and removal of these using linear regression.

At the single-subject level, voxelwise time series data were translated onto a surface representation of the cortex with 20,000 vertices, derived from

a macaque brain template [the F99 brain surface from CARET (38)]. Data at each vertex were normalized (such that the mean of the time series at each vertex was 0 and the variance was 1), and the global mean across the surface was regressed out at each vertex using linear regression. Finally, the mean time series for each Brodmann region in each hemisphere was obtained. Pairwise correlation coefficients (Pearson's *r*) for each pair of Brodmann areas (56 areas, 28 in each hemisphere) were calculated and transformed using Fisher's *r*-to-*z* transform.

ACKNOWLEDGMENTS. J.X.O. was funded by UK Medical Research Council (MRC) Biomedical Informatics Fellowship G0802459. P.L.C. was funded by the Charles H. Revson Foundation. S.J. was funded by the Wellcome Trust. C.R.E.W. was funded by Fondation Neurodis and a Marie Curie Intra-European Fellowship. R.B.M. was funded by UK MRC Research Grant G0802146. A.S.M. was funded by UK MRC Career Development Award G0800329. M.F.S.R., J.S., and M.P.N. were funded by UK MRC. M.G.B. and P.G.F.B. were funded by Wellcome Trust Grant 071291. The MRI scanner on which data were collected was funded by UK MRC Grant G0400593.

1. Biswal B, Yetkin FZ, Haughton VM, Hyde JS (1995) Functional connectivity in the motor cortex of resting human brain using echo-planar MRI. *Magn Reson Med* 34(4): 537–541.
2. Fox MD, Raichle ME (2007) Spontaneous fluctuations in brain activity observed with functional magnetic resonance imaging. *Nat Rev Neurosci* 8(9):700–711.
3. Hagmann P, et al. (2008) Mapping the structural core of human cerebral cortex. *PLoS Biol* 6(7):e159.
4. Smith SM, et al. (2012) Temporally-independent functional modes of spontaneous brain activity. *Proc Natl Acad Sci USA* 109(8):3131–3136.
5. Smith SM, et al. (2009) Correspondence of the brain's functional architecture during activation and rest. *Proc Natl Acad Sci USA* 106(31):13040–13045.
6. Friston KJ (2011) Functional and effective connectivity: A review. *Brain Connect* 1(1): 13–36.
7. Habas C, et al. (2009) Distinct cerebellar contributions to intrinsic connectivity networks. *J Neurosci* 29(26):8586–8594.
8. O'Reilly JX, Beckmann CF, Tomassini V, Ramnani N, Johansen-Berg H (2010) Distinct and overlapping functional zones in the cerebellum defined by resting state functional connectivity. *Cereb Cortex* 20(4):953–965.
9. Di Martino A, et al. (2008) Functional connectivity of human striatum: A resting state FMRI study. *Cereb Cortex* 18(12):2735–2747.
10. Roy AK, et al. (2009) Functional connectivity of the human amygdala using resting state fMRI. *Neuroimage* 45(2):614–626.
11. Zhang D, et al. (2008) Intrinsic functional relations between human cerebral cortex and thalamus. *J Neurophysiol* 100(4):1740–1748.
12. Filippini N, et al. (2009) Distinct patterns of brain activity in young carriers of the APOE-epsilon4 allele. *Proc Natl Acad Sci USA* 106(17):7209–7214.
13. Sorg C, et al. (2007) Selective changes of resting-state networks in individuals at risk for Alzheimer's disease. *Proc Natl Acad Sci USA* 104(47):18760–18765.
14. Supekar K, Menon V, Rubin D, Musen M, Greicius MD (2008) Network analysis of intrinsic functional brain connectivity in Alzheimer's disease. *PLOS Comput Biol* 4(6): e1000100.
15. Helmich RC, et al. (2010) Spatial remapping of cortico-striatal connectivity in Parkinson's disease. *Cereb Cortex* 20(5):1175–1186.
16. Wu T, et al. (2011) Functional connectivity of cortical motor areas in the resting state in Parkinson's disease. *Hum Brain Mapp* 32(9):1443–1457.
17. Hawellek DJ, Hipp JF, Lewis CM, Corbetta M, Engel AK (2011) Increased functional connectivity indicates the severity of cognitive impairment in multiple sclerosis. *Proc Natl Acad Sci USA* 108(47):19066–19071.
18. Roosendaal SD, et al. (2010) Resting state networks change in clinically isolated syndrome. *Brain* 133(Pt 6):1612–1621.
19. Anderson JS, et al. (2011) Functional connectivity magnetic resonance imaging classification of autism. *Brain* 134(Pt 12):3742–3754.
20. Li B, et al. (2013) A treatment-resistant default mode subnetwork in major depression. *Biol Psychiatry* 74(1):48–54.
21. Greicius MD, et al. (2007) Resting-state functional connectivity in major depression: Abnormally increased contributions from subgenual cingulate cortex and thalamus. *Biol Psychiatry* 62(5):429–437.
22. Bassett DS, et al. (2008) Hierarchical organization of human cortical networks in health and schizophrenia. *J Neurosci* 28(37):9239–9248.
23. Bassett DS, Nelson BG, Mueller BA, Camchong J, Lim KO (2012) Altered resting state complexity in schizophrenia. *Neuroimage* 59(3):2196–2207.
24. Honey CJ, et al. (2009) Predicting human resting-state functional connectivity from structural connectivity. *Proc Natl Acad Sci USA* 106(6):2035–2040.
25. Honey CJ, Kötter R, Breakspear M, Sporns O (2007) Network structure of cerebral cortex shapes functional connectivity on multiple time scales. *Proc Natl Acad Sci USA* 104(24):10240–10245.
26. Tyszka JM, Kennedy DP, Adolphs R, Paul LK (2011) Intact bilateral resting-state networks in the absence of the corpus callosum. *J Neurosci* 31(42):15154–15162.
27. Uddin LQ, et al. (2008) Residual functional connectivity in the split-brain revealed with resting-state functional MRI. *Neuroreport* 19(7):703–709.
28. Theyel BB, Llano DA, Sherman SM (2010) The corticothalamocortical circuit drives higher-order cortex in the mouse. *Nat Neurosci* 13(1):84–88.
29. Savazzi S, et al. (2007) Interhemispheric transfer following callosotomy in humans: Role of the superior colliculus. *Neuropsychologia* 45(11):2417–2427.
30. Adachi Y, et al. (2012) Functional connectivity between anatomically unconnected areas is shaped by collective network-level effects in the macaque cortex. *Cereb Cortex* 22(7):1586–1592.
31. Johnston JM, et al. (2008) Loss of resting interhemispheric functional connectivity after complete section of the corpus callosum. *J Neurosci* 28(25):6453–6458.
32. Quigley M, et al. (2003) Role of the corpus callosum in functional connectivity. *AJNR Am J Neuroradiol* 24(2):208–212.
33. Vincent JL, et al. (2007) Intrinsic functional architecture in the anaesthetized monkey brain. *Nature* 447(7140):83–86.
34. Mars RB, et al. (2011) Diffusion-weighted imaging tractography-based parcellation of the human parietal cortex and comparison with human and macaque resting-state functional connectivity. *J Neurosci* 31(11):4087–4100.
35. Sallet J, et al. (2011) Social network size affects neural circuits in macaques. *Science* 334(6056):697–700.
36. Brodmann K (1905) Beiträge zur histologischen Lokalisation der Grosshirnrinde. Dritte Mitteilung: Die Rindenfelder der niederen Affen. *J Psychol Neurol* 4:177–226.
37. Van Essen DC, Glasser MF, Dierker DL, Harwell J (2012) Cortical parcellations of the macaque monkey analyzed on surface-based atlases. *Cereb Cortex* 22(10):2227–2240.
38. Van Essen DC, et al. (2001) An integrated software suite for surface-based analyses of cerebral cortex. *J Am Med Inform Assoc* 8(5):443–459.
39. Damoiseaux JS, et al. (2006) Consistent resting-state networks across healthy subjects. *Proc Natl Acad Sci USA* 103(37):13848–13853.
40. Demeter S, Rosene DL, Van Hoesen GW (1990) Fields of origin and pathways of the interhemispheric commissures in the temporal lobe of macaques. *J Comp Neurol* 302(1):29–53.
41. Doty RW, Ringo JL, Lewine JD (1994) Interhemispheric sharing of visual memory in macaques. *Behav Brain Res* 64(1–2):79–84.
42. Sullivan MV, Hamilton CR (1973) Memory establishment via the anterior commissure of monkeys. *Physiol Behav* 11(6):873–879.
43. Foxman BT, Oppenheim J, Petito CK, Gazzaniga MS (1986) Proportional anterior commissure area in humans and monkeys. *Neurology* 36(11):1513–1517.
44. Risse GL, LeDoux J, Springer SP, Wilson DH, Gazzaniga MS (1978) The anterior commissure in man: Functional variation in a multisensory system. *Neuropsychologia* 16(1):23–31.
45. LaMantia AS, Rakic P (1994) Axon overproduction and elimination in the anterior commissure of the developing rhesus monkey. *J Comp Neurol* 340(3):328–336.
46. Livy DJ, et al. (1997) Increased axon number in the anterior commissure of mice lacking a corpus callosum. *Exp Neurol* 146(2):491–501.
47. Tovar-Moll F, et al. (2007) Neuroplasticity in human callosal dysgenesis: A diffusion tensor imaging study. *Cereb Cortex* 17(3):531–541.
48. Alstott J, Breakspear M, Hagmann P, Cammoun L, Sporns O (2009) Modeling the impact of lesions in the human brain. *PLOS Comput Biol* 5(6):e1000408.
49. Westlye ET, Lundervold A, Rootwelt H, Lundervold AJ, Westlye LT (2011) Increased hippocampal default mode synchronization during rest in middle-aged and elderly APOE ε4 carriers: Relationships with memory performance. *J Neurosci* 31(21): 7775–7783.
50. Wernicke C (1874) *Der aphasische Symptomencomplex. Ein psychologische Studie auf anatomischer Basis* (Cohn und Weigert, Breslau, Poland).
51. Geschwind N (1965) Disconnexion syndromes in animals and man. II. *Brain* 88(3): 585–644.
52. Geschwind N (1965) Disconnexion syndromes in animals and man. I. *Brain* 88(2): 237–294.
53. Catani M, Mesulam M (2008) The arcuate fasciculus and the disconnection theme in language and aphasia: History and current state. *Cortex* 44(8):953–961.
54. Warrington EK, Weiskrantz L (1982) Amnesia: A disconnection syndrome? *Neuropsychologia* 20(3):233–248.
55. Gaffan D, Hornak J (1997) Visual neglect in the monkey. Representation and disconnection. *Brain* 120(Pt 9):1647–1657.
56. Bartolomeo P, Thiebaut de Schotten M, Doricchi F (2007) Left unilateral neglect as a disconnection syndrome. *Cereb Cortex* 17(11):2479–2490.
57. He BJ, et al. (2007) Breakdown of functional connectivity in frontoparietal networks underlies behavioral deficits in spatial neglect. *Neuron* 53(6):905–918.
58. van Meer MP, et al. (2010) Recovery of sensorimotor function after experimental stroke correlates with restoration of resting-state interhemispheric functional connectivity. *J Neurosci* 30(11):3964–3972.
59. Smith SM, et al. (2004) Advances in functional and structural MR image analysis and implementation as FSL. *Neuroimage* 23(Suppl 1):S208–S219.
60. Woolrich MW, et al. (2009) Bayesian analysis of neuroimaging data in FSL. *Neuroimage* 45(1 Suppl):S173–S186.
61. Corballis MC (1998) Interhemispheric neural summation in the absence of the corpus callosum. *Brain* 121(Pt 9):1795–1807.
62. May PJ (2006) The mammalian superior colliculus: Laminar structure and connections. *Prog Brain Res* 151:321–378.
63. Paxinos G, Huang X-F, Petrides M, Toga A (2009) *The Rhesus Monkey Brain in Stereotaxic Coordinates* (Academic, London), 2nd Ed.